Fabrication of Nanoparticle Embedded Polymeric Microbeads as an Efficient Drug Delivery System

Geetanjali[1], Bhavani P. Nenavathu[2,*]

[1,2]*Department of Applied Sciences and Humanities, Indira Gandhi Delhi Technical University for Women, Delhi 110006, India*

*Corresponding author: E-mail: bhavaniprasadnaik@igdtuw.ac.in; Tel: (+91) 11-23900275

Received: 25 January 2019, Revised: 09 May 2019 and Accepted: 14 May 2019

DOI: 10.5185/amlett.2019.0003
www.vbripress.com/aml

Abstract

An efficient theragnostic which offers diagnosis and therapy of cancer is developed using a polymer based nanocarrier embedded with fluorescent quantum dots by the ionotropic gelation method. The FTIR spectra provide direct evidence of formation of polymer based nanocarrier comprising chitosan-alginate micro beads (CS-ALG beads). Notably, the SEM images showed highly porous structure of polymeric beads without Ag NPs and CdS QDs. The morphology of CS-ALG beads loaded with Ag NPs and CdS QDs showed smooth surface, glossy, homogenous shape under scanning electron microscopy and it could be due to high loading of fluorescent and silver NPs. The EDX analysis of as synthesised nanoparticle embedded polymeric beads showed X-ray peaks of Cd, S corresponds to CdS NPs. And the X-Ray peaks of C, O corresponds to the polymer beads. Characterization of nanocarrier for the presence of polymers has been confirmed by studies carried out using thermogravimetric analysis (TGA) showed complete degradation of Chitosan at about 450 °C while calcium alginate exhibits three-step decomposition. Further, the swelling studies of dried CS-ALG beads were carried out at room temperature and about 97% of swelling is being observed at pH 5 in 45 min. and 44% swelling is observed at pH 2.

Keywords: Chitosan-calcium alginate microbeads, silver nanoparticles, ionotropic gelation, drug delivery system, quantum dots.

Introduction

Majority of the gloal deaths are due to noncommunicable diseases (NCDS) and cancer caused the death of 9.5 million people in 2018. This data is based on the statistics produced by the International Agency for Research on Cancer (IARC) [**1**]. Generally, in many cases, tumor growth is detected at delayed stages and the use of radiation therapy and chemotherapeutic drugs at these stages are highly toxic to normal cells. So, it is necessary to recognize cancer at premature phase and drug delivery should be specific to the tumor site and drugs should be released in a controlled manner, which would control the growth of tumor [**2**]. In this aspect, controlled targeted drug delivery is used to investigate both diagnosis and treatment of cancer cells. Generally, a drug release system for cure of tumor should contain a carrier for loading the desired drug and tumor recognition site [**3, 4**]. However, currently many therapeutic agents used for the treatment of cancer suffer from the drawbacks such as poor solubility, toxicity and stability problems [**5, 6**]. To address this problem, many drug delivery systems (DDS) consisting of nanoparticles (NPs), polymer, microspheres, gels are used, not only to protect normal cells but also provide therapeutically effective drug concentrations at the tumor site [**7-10**].

In this aspect, Lee *et al.,* has fabricated gold nanoparticles immobilized with heparin and used them for detection and killing of metastatic tumor cells [**11**]. Asthana *et al.* has investigated the importance of polyamidoamine dendrimer as a release agent for controlled delivery of flurbiprofen drug [**12**]. Rajkumar *et al.* has conjugated doxorubicin, poly (ethylene glycol), folic acid to iron oxide nanoparticles and developed multi-functional nanocarriers for cancer therapy [**13**]. Luo-Yuan Li *et al.* have used naturally-occurring halloysite nanotubes as a nanocarrier for specific tumor site delivery of indocyanine green. Sanchita *et al.* has prepared calcium alginate beads using ionotropic gelation method, entrapped with trimetazidine drug [**14**]. Lindner *et al.* has developed lysolipid-based thermosensitive liposomes named hexadecylphosphocholine (HePC) as an effective drug release structure with rapid drug release induced by temperature [**15**]. Muller *et al.* has fabricated non-toxic nanocarriers solid lipid NPs (SLNs) using natural lipids or synthetic lipids [**16**]. Xubo Zhao *et al.* established a

drug release system using graphene oxide nanoparticles grafted by biocompatible PEGylated alginate with suitable size and shape [**17**]. Dhar *et al.* has fabricated single walled carbon nanotubes (SWCNTs) and conjugated with cisplatin-platinum (IV) prodrug and investigated its potential to target folic receptors positive tumor cells like human choriocarcinoma cells (JAr) and human nasopharyngeal carcinoma cells [**18**].

The objective of this study was to fabricate a theragnostic nanocarrier by embedding quantum dots (QDs) in to biopolymeric carrier. Here in, biopolymers such as alginate (ALG) and chitosan (CS) are made into suspension that serves as a template for the encapsulation and release of nanoparticles and drugs [**19**]. Alginate, a polysaccharide which is soluble in water and contains 1-4 linked a-L-guluronic acid and b-D-mannuronic acid residues. It has several unique properties like high gel porosity, dissolution and biodegradation under standard physiological environment [**20, 21**]. Chitosan is a linear polysaccharide, composed of (1-4)-linked 2-amino-2-deoxy-D-glucose (D-glucosamine) and 2-acetamido-2-Deoxy-D-glucose (N-acetyl-D-glucosamine) components. It has the property of gel formation and antimicrobial activity, which rendered them to use in designing of nanocarrier [**22**]**.** The more effective beads for the drug release could be formed by combining both ALG and the CS. The resultant CS-ALG micro beads are mechanically strong and are stable in acidic and neutral environment. Further, the as synthesized polymer based nanocarrier has been embedded with NPs which offer multi functionality, combining diagnostic (i.e., image contrast enhancement or tumor recognition ability achieved by using cadmium sulphide quantum dots (CdS QDs) and therapeutic features of silver nanoparticles (Ag NPs), a combination known as theragnostics. Silver nanoparticles possess antimicrobial activity and it works as an anti cancerous agent by reactive oxygen species (ROS) induced mechanism. Here in, Ag NPs and CdS QDs embedded CS-ALG beads are synthesized by ionotropic gelation method using in calcium chloride as a cross linking agent.

Experimental

Materials

Sodium sulphide (fused) flakes iron free, mercaptoacetic acid, toluene rectified, polyvinyl pyrrolidone K-25, was procured from Central Drug House (P) Ltd., India. Sodium acetate trihydrate, D – Glucose anhydrous, Sodium borohydride, Acetone, Sodium hydroxide pellets were procured from Thermo Fisher Scientific Pvt. Ltd., India. Cadmium chloride monohydrate 98%, sodium alginate are obtained from LOBA Chemie Pvt. Ltd., India. Distilled Water, Calcium chloride dihydrate were procured from Merck life Science Pvt. Ltd., India. Chitosan was obtained from SEZ Enterprise, India. Absolute ethanol (99.9%) was obtained from Changshu Hongsheng fine Chemical Co. Ltd., China. All the chemicals and solvents were used without further purification.

Fabrication of silver nanoparticles

Silver nanoparticles were synthesized by simple chemical reduction method using poly vinyl pyrrolidone (PVP) as a stabilizing agent. An aqueous solution of 0.01 M $AgNO_3$ was prepared and 1.5mg of PVP powder was added to it and continuously stirred for 35 min. Then $NaBH_4$ was to reduce silver ions in the solution mixture. The appearance dark brown colour of the solution indicates the formation of silver nanoparticles. The solution was stirred for 30min at room temperature and then Ag NPs were filtered and washed with deionised water and dried at 70^0 C [**23**].

Synthesis of CdS QDs

To 50 mM $CdCl_2$ aqueous solution, 87.2 µL of mercaptoacetic acid (MAA) dissolved in toluene was added drop wise. The above solution was stirred for 30 min. The pH of the resulting solution was raised to 8.0 using 0.1 N NaOH. Then the aqueous suspension of sodium sulphide was added and stirred for 3 h. The aqueous phase was separated and acetone was added to precipitate the CdS QDs. The CdS quantum dots (QDs) were separated by centrifuging at 4000 rpm for 5 min. The supernatant was discarded and the light-yellow colored precipitate so obtained was washed with deionized water. The supernatant was discarded and the residue comprising of MAA capped CdS QDs was stored till further used. This batch of sample will be henceforth referred to as CdS-MAA-QDs [**24**].

Preparation of chitosan alginate polymeric beads

Chitosan alginate (CS-ALG) polymeric beads were prepared by using ionotropic gelation technique. Initially, chitosan solution is prepared and $CaCl_2$ solution is added to it and the resultant mixture is stirred for 15 min. Then Na-alginate solution gradually added using a syringe and constantly stirred for 1 h at ambient temperature. The as-prepared beads were washed with deionised water and kept for air drying at room temperature.

Embedding of Ag NPs and CdS QDs in CS-ALG polymeric beads

An aqueous solution of silver nanoparticles is added to as synthesized CS-ALG beads and stirred for 2 h at room temperature, after that Ag NPs embedded polymeric beads were collected and washed with deionised water several times and air dried at room temperature. Further, these polymeric beads were added into the solution of cadmium sulphide quantum dots and stirred for 2 h at room temperature. Then, polymeric beads were collected and washed with deionised water and air dried overnight.

The concentrations of total NPs used and the free dispersed NPs in the dispersion obtained after synthesizing nanocarriers were determined using an ultraviolet (UV) spectrophotometer at a wavelength of 420 nm. The total NPs added (T, mg) for synthesizing nanocarriers and free dispersed NPs (D, mg).

$$\text{Encapsulation efficiency (EE \%)} = \frac{T-D}{T} \times 100$$

Swelling study

The Swelling studies of as synthesized polymeric beads were carried out at different pH ranging between 2 to 7. The dried beads were kept in buffer solution maintained at acidic (pH 2) and phosphate buffer (pH 5) and (pH 7) to simulate stomach and cancer cells and intestinal conditions respectively. Further accurately weighted amount (40 mg) of CS-ALG dried beads were kept in different pH solutions and stirred continuously at room temperature. After fixed time interval (5, 15, 30, 45 and 60 min.) beads were collected and smoothly wiped with the tissue paper and weighted. The dynamic weight change after fixed time interval and pH, defines the swelling degree (S*w*), and was calculated by the following equation.

$$Sw\ \% = \frac{Wt-Wo}{Wo} \times 100$$

where *Wt* is the weight of the beads after fixed time interval at time *t*, and *Wo* is the initial weight of the dry beads [**25**].

Characterization

The X-diffraction (XRD) measurements of the Ag NPs and CdS QDs were performed using powder diffractometer (M. Smartlab, Rigaku) operated at 40 KV using graphite monochromatized Cu K_α radiation source with a wavelength of 1.54 Å in a wide-angle region from 20° to 80° on a 2 θ scale. The optical properties of Ag NPs and CdS QDs were characterized by UV–visible spectrophotometer (Cary 100 UV Vis) in the range of 200–800 nm. The emission spectra of the above batches were measured by Shimadzu–RF–5301 PC fluorescence spectrophotometer in the range of 300-800 nm. The excitation and emission slit width of 5 nm was maintained for all the measurements. The thermal gravimetric analysis (TGA) was conducted on a Perkin-Elmer TGA 7- thermal analyzer from ambient to 800°C with a heating rate of 10°C min^{-1} under nitrogen atmosphere. The morphology of the Ag NPs and CdS QDs and surface characteristics of as synthesized beads were studied by scanning electron microscopy (VY.05) (SIGMA) operated at 5 KV. The sample preparation for scanning electron microscopy (SEM) measurement was done by spraying the dispersion of nanomaterials on a clean glass plate, dried at room temperature and coated with a thin layer of Au for electrical conductivity for incident electrons. Further, beads were mounted on metal stubs with conductive silver paint and sputtered with a thick layer of gold. Elemental composition of the imaged nanoparticles was determined by energy dispersive X-ray analyzer (EDAX) coupled to the SEM. The Swelling studies of the polymeric beads were studied by buffer solution at different pH. Fourier transform infrared (FT-IR) spectroscopy of the samples was conducted using KBr pellet method on a Bruker optic VERTEX 70v at room temperature in the range of 400-4000 cm^{-1}, to confirm the information about chemical bonds or functional groups present in the sample.

Results and discussion

The Ag NPs exhibited the typical surface plasmon resonance absorbance peak at wavelength 420 nm as shown in **Fig. 1a**, which confirms the formation of Ag NPs. The characteristic absorption peak of the MAA capped CdS QDs was observed at λabs = 411 nm as shown in **Fig. 1b**. Notably, the excitonic peak measured at 411nm for the batch of MAA capped CdS QDs corresponded to 2.8 nm particle size, measured by using effective mass approximation method and this data agreed well with the corresponding crystallite size of 2.6 nm measured by XRD. The band gap of CdS QDs was measured to be 3.01 eV. The fluorescence emission maximum of the MAA functionalized CdS QDs is obtained at 505 nm using λ_{exc} = 430 nm.

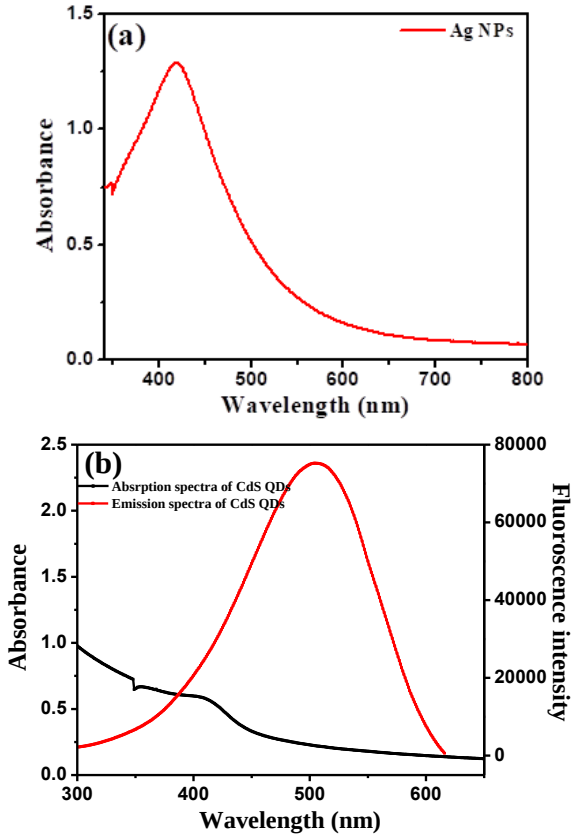

Fig. 1. (a) UV-vis absorbance spectra of silver nanoparticles. (b) Absorption (dashed) and emission (solid) spectra of MAA capped CdS Quantum dots. The characteristic absorption peak of the MAA capped CdS QDs is determined at 411nm and the corresponding maximum fluorescence emission is determined at 505 nm using λ ex = 430 nm.

The XRD pattern of the as-synthesized of Ag NPs revealed X-ray diffraction peaks at 2θ values of 37.76°, 44.18°, 64.22°, 77.10°, and 81.16° can be indexed as the (111), (200), (220), (311), and (222) crystal planes of the face-centred-cubic (FCC) phase of the Ag NPs as shown in **Fig. 2a**. The crystallite size was measured to be 18.70 nm for PVP capped Ag NPs and is in close agreement with previously reported literature for a = 4.086 Å, JCPDS 04-0783 [**26**]. Whereas for CdS QDs the X-ray diffraction peaks corresponding to 2θ values of 27°, 44° and 52° can be indexed as the (111), (220) and (311) crystal planes, and matched well with the cubic structure of CdS (JCPDS – file No. 10-454) shown in **Fig. 2b**. The average crystallite size was determined to be 2.6 nm. Our results were in good agreement with our previously reported literature [**27**]. The crystallite sizes (D) of Ag NPs and CdS QDs were estimated from peak broadening using Debye Scherrer formula $D = 0.89\ \lambda / \beta \cos\theta$; where λ is the wavelength of X-ray source, β is full-width at half maximum (FWHM) in radians and θ is Bragg's diffraction angle.

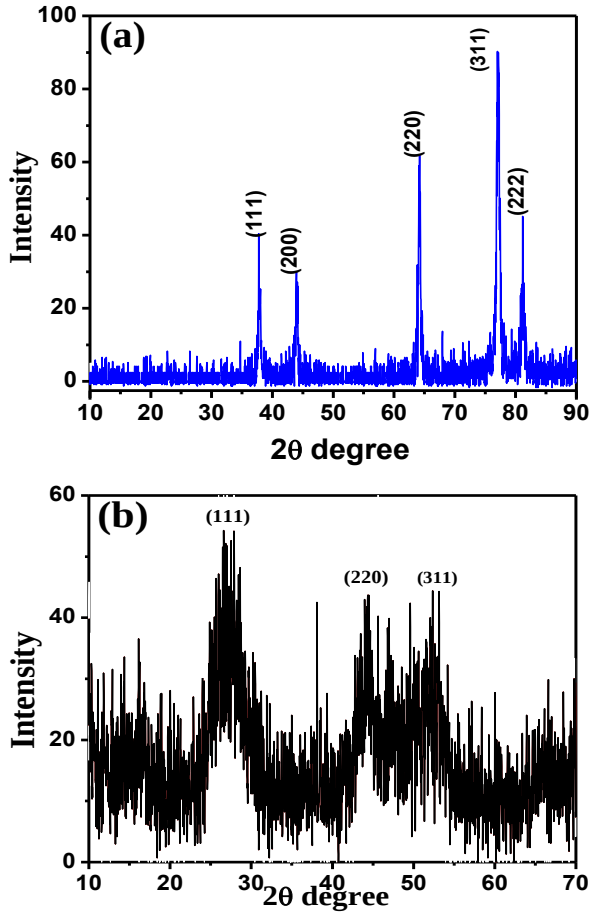

Fig. 2. (a) X-Ray diffraction (XRD) pattern of Ag NPs showing FCC (Face cubic centered) phase. (b) XRD Pattern of MAA capped CdS QDs.

The FTIR spectra provide direct evidence of formation of calcium alginate-chitosan micro beads. The appearance of band at 1738 cm^{-1} indicates the presence of carbonyl group in calcium alginate micro beads as shown in **Fig. 3a**. The band at 3600 cm^{-1} corresponds to stretching vibrations of OH groups and the bands at 1690 cm^{-1} and 1470 cm^{-1} corresponds to the vibrations of carbonyl bonds (C=O) of the amide group CONHR. The small peak at ~890 cm^{-1} corresponds to wagging of the saccharide structure of chitosan and absorption bands in the array from 1160 cm^{-1} to 1000 cm^{-1} has been ascribed to vibrations of CO group [**28, 29**].

Thermo gravimetric analysis (TGA) of CS-ALG beads showed that the primary degradation of both Chitosan and alginate beads at 100°C is due to loss of water molecules and further pure chitosan showed slight degradation at 220°C and completely degraded at about 450°C. While calcium alginate is decomposed in a series of 3 steps, in which 100.1°C corresponds to loss of water molecules and is subsequently degraded at 194°C, 648°C [**30, 31**]. The corresponding data is shown in **Fig. 3b**.

Further, the surface morphology of CS-ALG beads were studied by scanning electron microscopy which showed smooth surface, glossy, white and homogenously dispersed beads (Supplementary Fig. 1). Notably, the color of the Ca-alginate chitosan beads has been changed to brown after embedding Ag NPs and CdS QDs (Supplementary Fig. 2). Because of loss of water the beads there is shrinkage of beads and they lost their dimension.

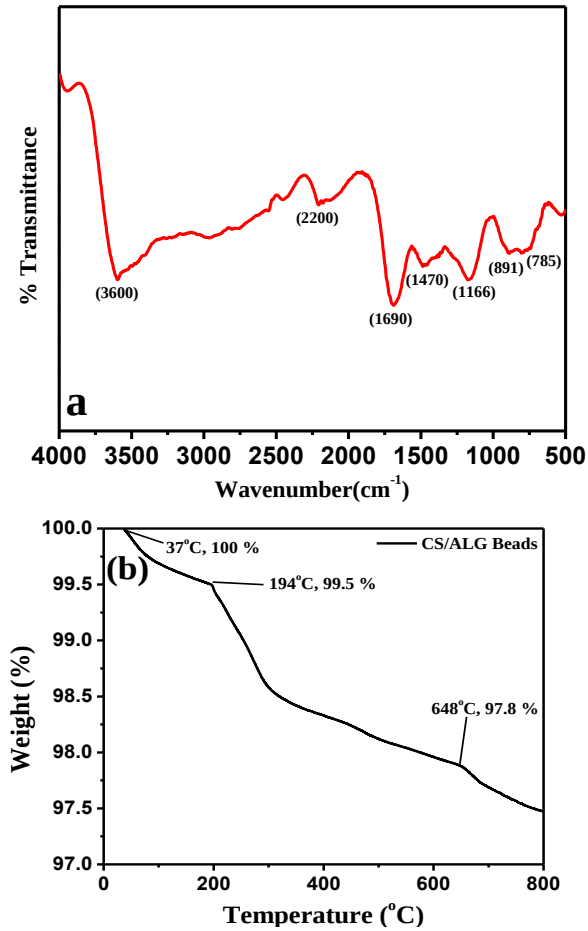

Fig. 3. (a) FTIR spectra in the 4000–400 cm^{-1} wave number range for chitosan/alginate beads. (b) TGA curves of chitosan/alginate beads.

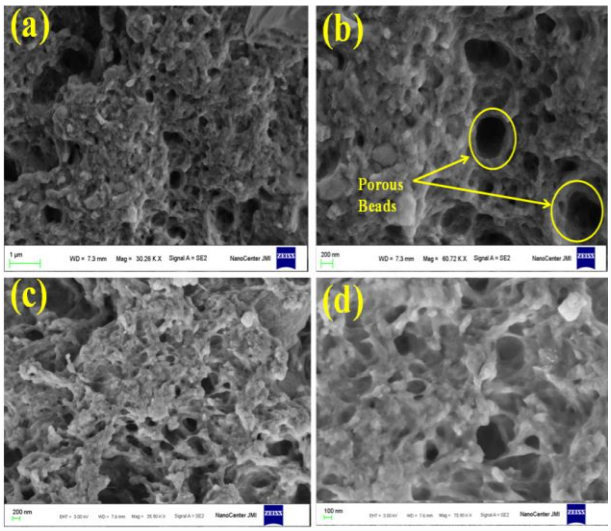

Fig. 4. (a), (b), (c) and (d) SEM images of chitosan/alginate beads showing porous morphology.

The SEM images shown in **Fig. 4a, b** revealed porous morphology of polymeric beads without Ag NPs and CdS QDs. These porous structures of the as synthesized polymeric beads provided excellent platform for the easy adsorption of Ag NPs and CdS QDs. The SEM image clearly showed the differences in surface morphology of both unloaded polymeric beads and nanoparticle embedded beads. Unloaded beads as shown in **Fig. 4c, d** represents porous morphology while nanoparticles loaded beads showed smooth surface as shown in **Fig. 5a, b** and **Fig. 6a, b, c, d** and **e** images. The **Fig. 6f** is the EDX analysis of as synthesised nanoparticle embedded polymeric beads, which revealed the X-ray peaks of Ag corresponding to Ag NPs and X-ray peaks of Cd, S corresponds to CdS NPs. And the X-Ray peaks of C, O corresponds to the polymer beads. The presence of divalent metal ions such as Ca^{2+}, Cd^{2+} contributed to the transformation of alginate from sol in to gel by cross-linking the alginate. In addition to these cations in the solution, guluronic acid also played major role in the development of porous gel [**32**].

The particle sizes of the beads prepared by using sequential method are measured to be in the range of 500 µm to 550 µm. The schematic illustration for the formation of chitosan/alginate beads embedded with Ag NPs and CdS quantum dots is shown in supplementary Fig. 3. The swelling studies of dried polymeric beads were carried out at room temperature and about 97% of swelling is being observed at pH 5.0 in 45 min. and 44% at pH 2.0 as shown in the **Fig. 7**. The presence of primary amino groups on the chitosan backbone contributed for the design of polysaccharide based targeted nanocarriers. The polyelectrolyte complex is formed by the ionic interaction between the carboxyl residue of alginate and the amino residue of chitosan. This polyelectrolyte complex can be extensively used to attain nanocarriers for the controlled delivery of drugs.

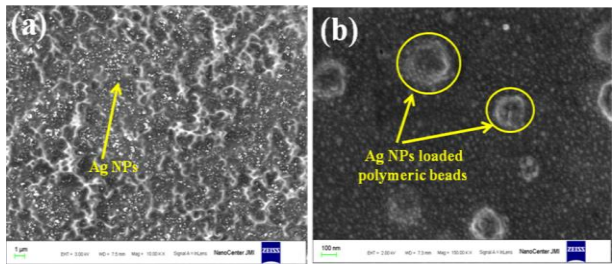

Fig. 5. (a), (b) SEM images showing embedding of Silver nanoparticles in Polymeric beads.

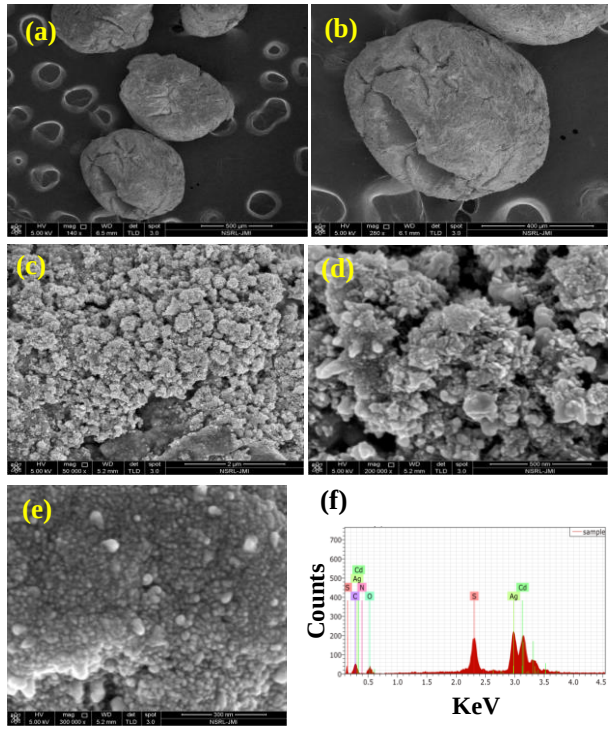

Fig. 6. (a), (b), (c), (d), (e) SEM images showing of chitosan/alginate beads embedded with both Ag NPs and CdS QDs acting as a theragnostic and (f) Energy dispersive X-ray analysis of a representative nanocarrier showing Ag corresponding to Ag NPs and X-ray peaks of Cd, S corresponds to CdS NPs and the X-Ray peaks of C, O corresponds to the polymer beads.

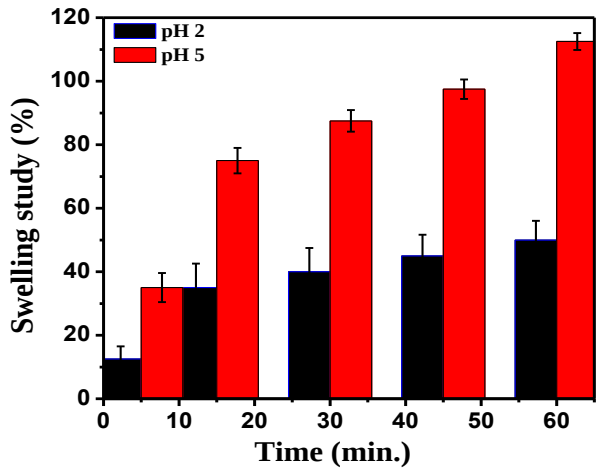

Fig. 7. Effect of pH on the swelling of chitosan/alginate beads.

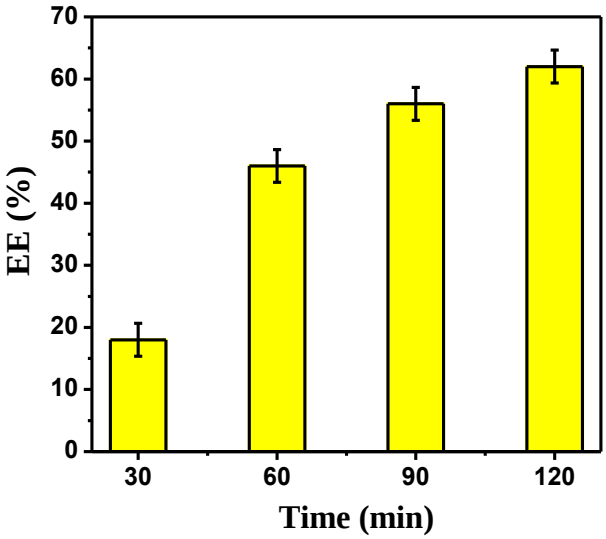

Fig. 8. Effect of time on the Ag NPs encapsulation efficiency of chitosan/alginate beads.

The pH of the buffer solution is the prominent feature causing the swelling ratio of the beads [**33**]. The as synthesized CS/ALG beads showed low swelling index in acidic pH and the likely reason could be due to the movement of solvent in to the highly polymerized gel through formation of alginic acid residues. At the pH of (1.2), the CS/ALG molecules remain un-ionized [**34**]. Further movement of solvent in to the network is prevented resulting in decrease in swelling of the beads. However, the presence of hydrophilic groups in the polymeric beads contributed to the diffusion of water through the minute opening on the surface of the beads and resulted in insignificant swelling in the acidic medium. In addition, the beads obtained by adding alginate polymer showed higher swelling behavior. However, when alginate is added, it protected the CS polymer chains from instantaneous enlargement and collapse of beads. When the pH of the solution is above the pKa of the polymer, the carboxylic groups present in the polymer are deprotonated and resulted in the formation of ($-COO^-$), with enhancement in the repulsion between negative charges. This enhanced the electrostatic repulsive force between the polymer chains and resulted in water inclusion and a higher swelling ratio. When the pH of the solution in which the beads are placed is maintained above the pKa of ALG, results in high swelling ratio and the swelling nature would increase with increase in the pH value. When the beads came in to contact with the buffer solution at pH > 7 lead to increase in the electrostatic repulsive force between the residues in the polymer chains and caused dissolution of the bead structure. The collapse of the CS/ALG in pH > 7 would make a huge contribution to the rapid drug release in intestinal and stomach, colon-specific drug delivery system. Notably the collapse of the beads has been observed at pH >7. For proper loading and releasing of a drug, the alginate beads should take up solvent and swell considerably. The as synthesized beads possibly swell up to some extent in the stomach and in the upper intestine and lower intestine; they may swell significantly based on the respective pH conditions maintained. The as synthesized micro beads possess a high porous gel structure which favors high drug loading and dissolve and biodegradation of the nanocarrier under regular physiological environment. Herein, the encapsulation efficiency (EE %) of the as synthesized nanocarrier was found to be increasing with increase in time. **Fig. 8**. shows that the NPs encapsulation efficiency increased slightly from 18% to 62%, with increase in time. In the first 30 min., 18% EE% was observed. Further it is increased to 46% in 60 min and 56% in 90 min. and reached up to 62 % in 2h. On the whole, it was obvious that the NPs encapsulation increased from 18% to 62% in 2h.

Theragnostics have the ability to monitor effectiveness of therapeutic response, thus expediting therapeutic decisions while improving patients' life-quality [**35**]. The as synthesized multifunctional delivery system is co-loaded with CdS quantum dots which act as diagnostic agent and Ag NPs for attaining therapeutic effect. QDs are immensely attractive fluorophores for in vivo imaging in living organisms [**36**]. They are resistant to photobleaching and possess high level of brightness [**37**].

Further, it is widely investigated that Ag NPs has the ability to kill the cancer cells. Foldbjerg *et al.* investigated that polyvinyl pyrrolidone coated nano-Ag induced cytotoxicity and genotoxicity and mitochondrial damage and early apoptosis was observed in the human alveolar cell line A549 through reactive oxygen species (ROS) formation [**38**]. Ag NPs inhibited the proliferation and apoptosis is enhanced in keratinocytes, liver cells, lung cells, macrophages, and Jurkat T cells [**39-44**].

Conclusion

To summarize, we fabricated CS-ALG microspheres and further we embedded these beads with silver nanoparticles and CdS QDs. This novel pH-sensitive multifunctional delivery system co- loaded with CdS quantum dots which act as diagnostic agent and Ag NPs for attaining therapeutic effect. The presence of carboxylic and hydroxyl groups in the polymer network favours the load of high concentration of drugs and nanoparticles in to the beads. The NPs encapsulation efficiency in CS/ALG beads was observed to be 62% in 2h at the conditions of 2.5% w/v ALG and 0.2% w/w CS. The swelling behaviour of the beads is pH dependent. The beads swell slightly pH 1.2, but swelling gradually increases at pH 5. The nanoparticle loaded beads of alginate mixed with chitosan are nontoxic, biodegradable and biocompatible and may be used as an efficient controlled targeted drug delivery system and is used to investigate both diagnosis and killing of cancer cells.

Acknowledgment

The authors are thankful to Indira Gandhi Delhi Technical University for Women for providing the facilities. The authors also give thanks to the Jamia Millia Islamia, New Delhi for providing the instrumental facilities. This work has been carried out under the Science and Engineering Research Board (SERB), grant no. EEQ/2016/00616 and the authors are thankful to the SERB for the financial support. Geetanjali is grateful to Science & Engineering Research Board (SERB), Government of India for funding fellowship.

Author's contributions

Conceived the plan, Data analysis, Wrote the paper. Authors have no competing financial interests.

References

1. Freddie, B.; Jacques, F.; Isabelle, S.; R. L. S.; L. A. T.; Ahmedin, J.; *Ca. Cancer. J. Clin.* **2018**, *68*, 424.
2. Liang, X. J.; Chen, C.; Zhao, Y.; Wang, P. C., *J. Methods Mol. Biol*. **2010**, *596*, 488.
3. Kumar, B.S.; Mol, L.A.; *J. Inter Scholarly Res Notices*, **2014**.
4. Fakhar, U.; Waqar, A.; Izhar, U.; Omer, S.Q.; Omer, M.; Shumaila, S.; Alam, Z.; *Int. J. Nanomedicine.*, **2017**, *12*, 7309.
5. Mishra, R.D.K.; *Int. J. Nanomedicine*., **2008**, *3*, 274.
6. Kanika, M.; Sandeep, K.; Neelam, P.; Viney, L.; Deepti, P.; *J. Pharm. Bioallied. Sci*., **2014**, *3*, 150.
7. Wim, D.J.; Paul, J.A.B.; *Int. J. Nanomedicine.*, **2008**, *2*, 149.
8. Sarabjeet, S.S.; Hicham, F.; Baljit, S.; *J. Occupational Medicine and Toxicol.*, **2007**, *2*, 6.
9. Farnaz, A.; Hoda., J.M.; Mossein, A.; Hamideh, V.; Navideh, A.; Omid, A.; Aydin, B.; *J. Critical Reviews in Biotech*., **2017**, *37*, 509.
10. Jitendra N.; Nano based drug delivery, IUPAC Publishing Zagreb, Croatia, **2015**.
11. Lee, K.; Lee, H.; Bae, K.H.; Park, T.G.; *J. Biomaterials*., **2010,** *25*, 6536.
12. Abhay, A.; Abhay, S.C.; Prakash, V.D.; Narendra, K.J.; *J. AAPS. Pharm. Sci. Tech.*, **2005**, *3*, E542.
13. Rajkumar, S.; Prabaharan, M.; *J. Colloids Surf. B Biointerfaces.*, **2018**, *170*, 537.
14. Sanchita, M.; Senthil, K.S.; Balakrishnam, K.; Sanat, K.B.; *J. Pharmaceutical Science*. **2010**, *46*, 793.
15. Lindner, L.H.; Hossann, M.; Vogeser, M.; Teichert, N.; Wacholz, K.; Hiddemann, W.; Issels, R.D.; *J. Control. Release*, **2008**, 125, 793.
16. Mukherjee, S.; Ray, S.; Thankur, R.S.; *Indian J. Pharm. Sci*. **2009**, *71*, 358.
17. Zhao, X.; Liu, L.L.; Zeng, J.; Jia, X.; Liu, P.; *Langumuir J.*, **2014**, *34*, 10429.
18. Huiling, M.; Rene, H.; *J. Expert opinion on Drug Delivery*, **2018**, *15*, 785.
19. Rajan, S.B.; Nagasamy, V.D.; Ayush, S.; *J. Chronicles of Young Scientists*, **2011**, *2*, 196.
20. Joby, J.; Jozef, T.H.; Sabu, T.; Sreeraj, G.; *Materials Today Chemistry*, **2018**, *9*, 55.
21. Aysu, Y.; Ferhan, S.; *J. Chem. Parm. Res*., **2010**, *3*, 721.
22. Sinha, V.R.; Singla, A.K.; Wadhawan, S.; Kaushik, R.; Kumri, R.; Bansal, K.; Dhawan, S.; *International J. of Parmaceutical*, **2004**, *274*, 33.
23. Slistan, G.; Herrera, U. A.; Rivas, S. R.; Avalos, B.J.F.; Castillon, B. M.; *J. Material. Research. Bulletin.*, **2008**, *43*, 96.
24. Bhavani, P. N.; Raj, K. D.; *J. Adv. Mat. Lett.*, **2013**, *5*, 362.
25. Lorena, S.; Lorella, G.; Paolo, M.; Franco, P.; *J. Scientifica* **2016**, *2016*, 8.
26. Hyeong, H. P.; Xin, Z.; Yong, J. C.; Hyung, H. P.; Ross, H.H.; *J. of Nanomaterials*, **2010**.
27. Qutub, N.; Sabir, S.; *Int. J. Nanosci. Nanotechnol.*, **2012**, *2*, 120.
28. Ping, L.; Ya, N. D.; Jun, P. Z.; Ai, Q. W.; Qin, W.; *Int. J. Biomed. Sci*., **2008**, *4*, 228.
29. Xu, Y.X.; Kim, K.M.; Hanna, M.A.; Nag, D.; *Industrial Crops and Products*, **2005**, *21*, 192.
30. Rana, V. K.; Asutosh, K. P.; Raj, P. S.; *J. Macromolecular Research*, **2010**, *18*, 720.
31. Shamshina, J.L.; Gurau, G.; Block, L.E.; Hansen, L. K.; *J. Mater. Chem. B*, **2014**, *2*, 3936.
32. Rajinikanth, P.S.; Sankar, C.; Mishra, B.; *Drug Delivery*, **2003**, *10*, 28.
33. Hanne, H. T.; Jan, K.; *J. Drug Development and Industry Pharmacy*, *28*, 630.
34. Raffin, F.; Duru, C.; Jacob, M.; *Int. J. Pharm.*, **1996**, *145*, 252.
35. Jabr-Milane, L.; Van Vlerken, L.; Devalapally, H.; Shenoy, D.; Komareddy, S.; Bhavsar, M.; Amiji, M.; *J. Control. Release*, **2008**, 130, 128.
36. Zdobnova, T.A.; Lebedenko, E.N.; Deyev, S.M.; *Acta Naturae*, **2011**, 3, 47.
37. Green, N.M.; *Methods Enzymol.*, **1990**, 184, 67.
38. Foldbjerg, R.; Dang DA.; Autrup H.; *Arch Toxicol*., **2011**, *85*, 50.
39. Yen, H. J.; Hsu, S. H.; Tsai, C. L.; *Small*, **2009**, *5*, 1561.
40. Eom, H. J.; Choi, J.; *Environ. Sci. Technol.*, **2010**, *44*, 8842.
41. Lee, Y. S.; Kim, D. W.; Lee, Y. H.; Oh, J. H.; Yoon, S.; Choi, M. S.; Lee, S. K.; Kim, J. W.; Lee, K.; Song, C. W.; *Arch. Toxicol*., **2011**, *85*, 1540.
42. Piao, M. J.; Kang, K. A.; Lee, I. K.; Kim, H. S.; Kim, S.; Choi, J. Y.; Choi, J.; Hyun, J. W.; *Toxicol. Lett.*, **2011**, *201*, 100.
43. Zanette, C.; Pelin, M.; Crosera, M.; Adami, G.; Bovenzi, M.; Larese, F. F.; Florio, C.; *Toxicol. In Vitro*., **2011**, *25*, 1060.
44. Lim, D. H.; Jang, J.; Kim, S.; Kang, T.; Lee, K.; Choi, I. H.; *Biomaterials.*, **2012**, *33*, 4699.

